ChemPubSoc Europe

DOI: 10.1002/chem.201504591

CHEMISTRY A European Journal Full Paper

Biosensors

Design of an Os Complex-Modified Hydrogel with Optimized Redox Potential for Biosensors and Biofuel Cells

Piyanut Pinyou[+],[a] Adrian Ruff[+],[a] Sascha Pöller,[a] Su Ma,[b] Roland Ludwig,[b] and Wolfgang Schuhmann*[a]

Abstract: Multistep synthesis and electrochemical characterization of an Os complex-modified redox hydrogel exhibiting a redox potential $\approx +30$ mV (vs. Ag/AgCl 3 M KCl) is demonstrated. The careful selection of bipyridine-based ligands bearing *N*,*N*-dimethylamino moieties and an amino-linker for the covalent attachment to the polymer backbone ensures the formation of a stable redox polymer with an envisaged redox potential close to 0 V. Most importantly, the formation of an octahedral N6-coordination sphere around the Os central atoms provides improved stability concomitantly with the low formal potential, a low reorganization energy during the $Os^{3+/2+}$ redox conversion and a negligible impact on oxygen reduction. By wiring a variety of enzymes such as pyrroloquinoline quinone (PQQ)-dependent glucose dehydrogenase, flavin adenine dinucleotide (FAD)-dependent glucose dehydrogenase and the FAD-dependent dehydrogenase domain of cellobiose dehydrogenase, low-potential glucose biosensors could be obtained with negligible co-oxidation of common interfering compounds such as uric acid or ascorbic acid. In combination with a bilirubin oxidase-based biocathode, enzymatic biofuel cells with open-circuit voltages of up to 0.54 V were obtained.

Introduction

Wiring of enzymes to electrode surfaces by means of redox hydrogels[1] is of particular interest for the design of biosensors,[2–4] enzymatic biofuel cells[5–7] or biophotovoltaic devices.[8–10] The electron transport between the electrode and the prosthetic group of the enzyme within these bioactive films is mediated by redox relays that are attached to the hydrogel backbone. Osmium complexes of the type $[Os(bpy)_2L_x]$ (bpy = 2,2′-bipyridine, L = chloro ligand or ligand bearing a linker group for the attachment to the polymer backbone; $x = 1$, 2) are widely used as redox mediators in hydrogels because of the fast electron transfer rates they exhibit between the Os centers and the prosthetic groups in various enzymes, for example, among others glucose oxidase,[11–13] PQQ-dependent glucose dehydrogenase (PQQ-sGDH, PQQ = pyrroloquinoline quinone),[14,15] cellobiose dehydrogenase (CDH),[16,17] pyranose dehydrogenase[18] or laccase.[19] Moreover, the formal potential of these complexes can be tuned by the introduction of appropriate electron-withdrawing or electron-donating groups into the ligand sphere.[15,18,20–22]

For glucose sensors, low operating potentials, which are determined by the redox potential of the used mediator, are preferred to avoid interferences caused by electrochemically induced side reactions, for example, the oxidation of ascorbate or urate.[23,24] Moreover, low potential anodes ensure a high open-circuit voltage in glucose-based biofuel cells, which is determined by the difference between the potentials of the bioanode and the biocathode.[25]

One strategy to synthesize Os-based redox mediators with low formal potentials is the introduction of chloro ligands to the inner ligand sphere of the Os-complexes (L = Cl). Following this approach, redox potentials < 0 V (vs. Ag/AgCl 3 M KCl) can be achieved. However, the chloro ligands are labile and tend to undergo ligand exchange reactions with solvent molecules, the electrolyte, or functional groups (e.g., carbonyl or carboxyl groups) at the polymer backbone. Moreover, unintended ligand exchange reactions can be induced electrochemically upon oxidation or reduction of the transition-metal center. This effect was used for electrochemical induced crosslinking of the polymer chains that bear free pyridine ligands to produce stable and dense films at the electrode surface.[26,27] However, these active layers contain Os complexes with different ligand spheres and hence different formal potentials if the ligand exchange is not complete and/or Os complexes with different ligands are formed.[26] Moreover, the electron diffusion coefficient within such polymers is low as compared to redox hydrogels that bear redox relays bound through flexible linkers.[28,29]

[a] *P. Pinyou,[+] Dr. A. Ruff,[+] Dr. S. Pöller, Prof. Dr. W. Schuhmann*
Analytical Chemistry
Center for Electrochemical Sciences (CES)
Ruhr-Universität-Bochum, Universitätsstrasse 150
44780 Bochum (Germany)
E-mail: wolfgang.schuhmann@rub.de

[b] *Dr. S. Ma, Dr. R. Ludwig*
Department of Food Sciences and Technology
Vienna Institute of Biotechnology, BOKU - University of Natural Resources and Life Sciences, Muthgasse 11/1/56; 1190, Vienna (Austria)

[+] *These authors contributed equally to this work.*

Supporting information and the ORCID identification number(s) for the author(s) of this article can be found under http://dx.doi.org/10.1002/chem.201504591.

Other approaches for the formation of low potential Os complexes use the introduction of NO ligands, that is, imidazole derivatives that contain ester groups. The coordination takes place through the O atom of the carbonyl group and the imino N atom in the imidazole ring.[15,17,30] However, the coordinative O–Os bond is labile and again ligand exchange reactions with solvent molecules[31] and functional groups within the polymer chain may occur. This leads again to species with a variety of different redox potentials.[15,17] Thus, an Os complex with six N coordination sites would be preferable.

Osmium complexes with ligand spheres based on *N*,*N*′-dialkylated-2,2′-diimidazole derivatives exhibit also remarkable low redox potentials (< -150 mV vs. Ag/AgCl 3 M KCl).[15,29] However, these complexes reveal redox potentials that invoke the catalytic reduction of oxygen by the polymer-bound redox mediator itself ($< +70$ mV vs. Ag/AgCl 3 M NaCl).[32] Hence, the application in biosensors and biofuel cells that are operated under ambient conditions avoiding parasitic reduction currents at the bioanode is hampered.

Recently, we described the synthesis of an Os complex bearing two bipyridyl (bpy) ligands and an ethylenediamine-modified bpy ligand for the modification of a poly(methacrylate)-based polymer backbone by reacting epoxy groups introduced in the polymer backbone and the $-NH_2$ group at the bpy derivative.[33] This redox polymer revealed a high chemical stability even under harsh conditions (pH 3). However, the polymer showed a rather high redox potential of $+0.64$ V versus Ag/AgCl 3 M KCl.[33]

To decrease the potential of the $Os^{3+/2+}$ couple, electron-donating groups need to be introduced at the bpy-based ligand system.[22] The synthesis of such low-potential Os complexes were first reported by Heller et al. in 2003[20,29] and later optimized by Leech et al.[21,34] The authors introduced amino groups in the *para* positions to the coordinating N-atoms in the bpy ligands. Os complexes bearing two diamino-modified bpy ligands and two chloro ligands show a formal potential of -0.57 V (vs. Ag/AgCl 3 M KCl).[21] Obviously, the introduction of electron-donating groups leads to a strong decrease in the redox potential of the corresponding Os complexes. However, these complexes were decomposed by oxidation of the introduced amino moieties.

In this paper, we suggest the design of a new, highly-stable, and low-potential Os complex overcoming limitations such as unstable ligand sphere, unstable electron-donating substituents, as well as catalytic activity for oxygen reduction or interference oxidation. A N6-coordination sphere is envisaged, avoiding any labile chloro or oxygen coordination. Dimethylamino groups are used as stable electron-donating groups in *para* position to the N-coordination sites of bpy ligands. One of the bpy ligands additionally carries an amino-terminated flexible linker that allows binding to a copolymer backbone for the formation of the corresponding redox hydrogels. By integration of a variety of enzymes such as PQQ-dependent glucose dehydrogenase, FAD-dependent glucose dehydrogenase, and the FAD-containing dehydrogenase domain of cellobiose dehydrogenase, low-potential glucose biosensors and bioanodes for biofuel cells were obtained and characterized.

Results and Discussion

Synthesis of the Os complex-based redox mediator

The use of amino-modified bpy ligands ensures low redox potentials.[20,29] However, the free amino groups in the outer sphere of such ligands may react randomly with epoxy functions at the polymer backbone. This leads finally to a number of various products with different degree of binding (i.e., number of reacted amino groups). In addition, the large number of $-NH_2$ groups at the Os complex may induce unintended crosslinking reactions between different polymer chains already formed during the polymer modification process. Furthermore, the $-NH_2$ groups attached to bpy tend to undergo oxidation even at ambient conditions, which would cause to a change in the redox potential of the polymer-bound Os complex. Dimethyl amino groups ($-NMe_2$) provide an even stronger donor effect than the $-NH_2$ group ($+$I effect of the methyl groups). Hence, bpy ligands carrying $-NMe_2$ groups instead of $-NH_2$ groups should ensure a low redox potential of the corresponding Os complex. Moreover, the $-NMe_2$ functions are inactive during the attachment of the complex to the polymer backbone through a ring-opening reaction of the polymer-bound epoxy groups at mild conditions. Anchoring of the Os complex to the polymer chain is only due to the reaction between the predefined binding site at the polymer backbone and a corresponding linker species (see below). Furthermore, *N*,*N*′-dimethylaniline species are inert against oxidation through molecular oxygen under ambient conditions.[35]

A suitable $-NMe_2$-modified bpy was synthesized starting from *N*,*N*-dimethylamino pyridine (DMAP, **1**, Scheme 1). The pyridine precursor DMAP was first treated with $[Sn(n\text{Bu})_3Cl]$ to form the pyridyl stannate **2**. Treatment of **1** with *n*BuLi, followed by treatment with I_2 leads to halide **3**. Finally, the Pd^0-catalyzed Stille cross-coupling between stannate **2** and halide **3** gives the $-NMe_2$-modified bpy ligand **dmabpy** in 76% yield.[36]

The Os^{2+}-dichloro complex **5** is obtained by treating **dmabpy** and K_2OsCl_6 in dimethylformamide (DMF) at high temperatures followed by the reduction of the Os species to Os^{2+} with $Na_2S_2O_4$ in water (Scheme 1).[37] Cyclic voltammo-

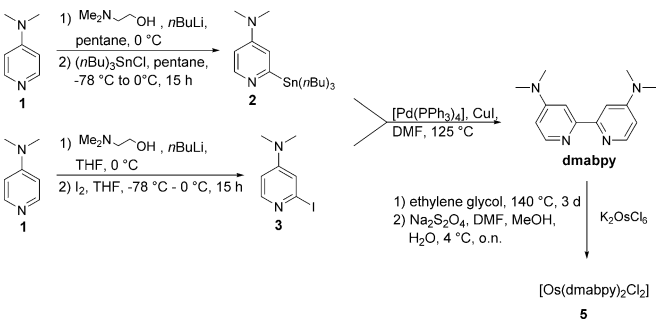

Scheme 1. Synthesis of Os complex **5** $[Os(\textbf{dmabpy})_2Cl_2]$ by treating **dmabpy** with K_2OsCl_6 in ethylene glycol. The **dmabpy**-ligand was synthesized through the cross-coupling of stannate **2** and the iodo compound **3** starting from DMAP (**1**) based on protocols described in ref. [36].

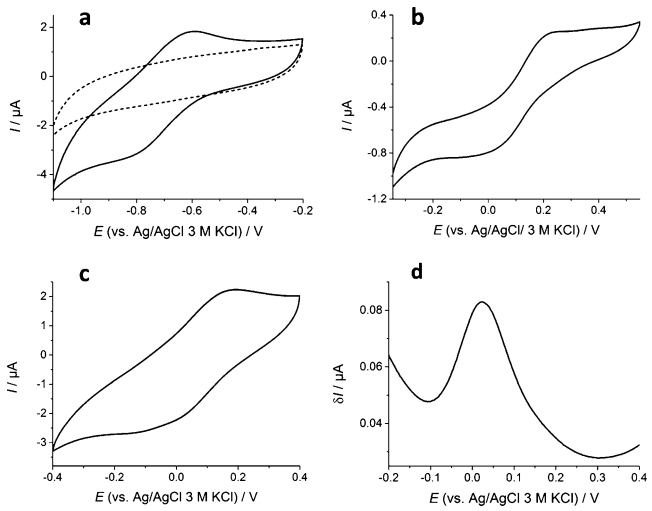

Figure 1. Voltammetric characterization of Os complexes **5** (a) and **12** (b) as well as the redox polymer **P-12** (c and d); a) cyclic voltammograms in the potential window of −1.1 to −0.2 V (vs. Ag/AgCl 3 M KCl) of **5** (——) in 0.1 M KCl/water drop-coated from EtOH onto a GC electrode (diameter = 3 mm); the dashed line corresponds to the *I/E* curve recorded with the bare GC electrode; scan rate = 100 mV s^{-1}; b) cyclic voltammogram of **12** in 0.15 M NBu_4PF_6/MeCN at a Pt electrode (1 mm), scan rate = 50 mV s^{-1}c: cyclic voltammogram of **P-12** drop-cast onto a graphite electrode (3.05 mm) in PBS buffer (pH 7.4); d) differential pulse voltammogram of **P-12** in 3 M KCl/water deposited onto a Pt electrode (1 mm); pulse amplitude = 15 mV, pulse width = 0.06 s

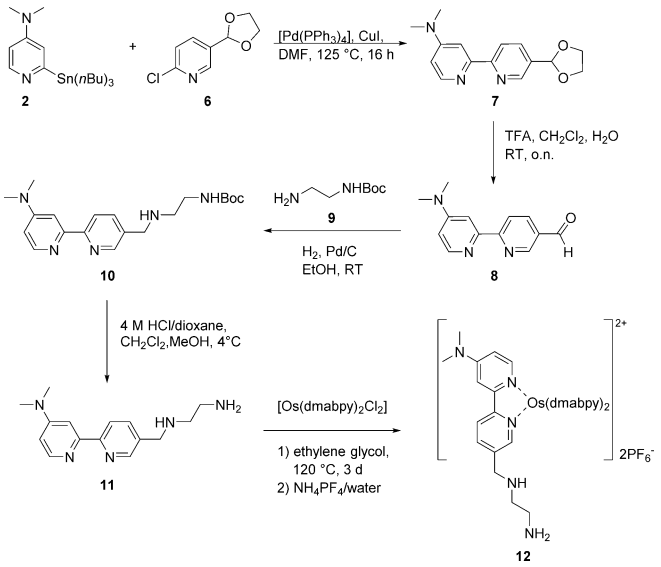

Scheme 2. Multistep synthesis of complex **12** starting from DMAP and acetal **6** (see the Supporting Information for synthesis of **6**). The target compound is obtained as the hexafluorophosphate salt through a metathesis reaction with NH_4PF_6 in water.

grams in the potential range of −1.1 to −0.2 V (vs. Ag/AgCl 3 M KCl) of **5** deposited onto a glassy carbon (GC) electrode in 0.1 M KCl/water reveal a chemically reversible redox couple with a half-wave potential $E_{1/2}$ of −0.70 V (vs. Ag/AgCl 3 M KCl, Figure 1a, ——). Compared with the previously known $-NH_2$-modified complex (−0.57 V vs. Ag/AgCl 3 M KCl, adsorbed on a GC electrode in 0.1 M phosphate buffer solution), this value is shifted to even more negative potentials ($\Delta E = -130$ mV) as expected from the stronger electron-donating effect of the bpy-bound *N,N′*-dimethylamino groups. Voltammograms recorded with a bare electrode in the same potential range show no redox signals (Figure 1a, -----). Voltammetric characterization of **5** in solution was conducted in 0.15 M NBu_4BF_4/MeCN at a Pt electrode. The *I/E* curve (not shown) of **5** shows a chemically reversible redox couple with an estimated half-wave potential of $E_{1/2} = -0.63$ V (vs. Ag/Ag^+ 0.01 M $AgClO_4$). This value is shifted to higher potentials compared with the value obtained in aqueous electrolytes. However, the use of different reference electrodes prevents a direct comparison of the measured redox potentials.

Recently, we described the synthesis of an amino-modified bpy-ligand (bpy_{amino}) suitable for the attachment to an epoxy-modified polymer backbone by a ring-opening reaction between the nucleophilic $-NH_2$ and the anchoring group.[33] This ligand was synthesized starting from 2-bromopyridine and acetal **6** (Scheme 2; for the synthesis of **6** see Scheme S1 in the Supporting Information and ref. [30]). Ligand exchange with $[Os(bpy)_2Cl_2]$ leads to the complex $[Os(bpy)_2(bpy_{amino})]^{2+}$. The complex showed high stability and was used as internal potential standard in a miniaturized pH sensor over a wide pH range. However, as expected, due to the absence of any electron-donating groups at the bpy ligands, the redox potential of the $[Os(bpy)_2(bpy_{amino})]^{2+}$ complex is +0.64 V versus Ag/AgCl 3 M KCl (note, the redox potential of $[Os(bpy)_2Cl_2]$ is ≈0 V).

To retain the redox potential of the Os-complex as low as possible we exchanged the 2-bromopyridine precursor in our earlier published synthesis[33] by DMAP, which contains a $-NMe_2$ group in *para* position to the coordinating N-atom. Cross-coupling of stannate **2** (synthesized from DMAP in two steps through **3**; see the Supporting Information) and **6** gives bipyridine **7** in good yield (91%). Deprotection under acidic conditions leads to the carboxaldehyde **8**. Reductive amination with mono-protected ethylene diamine **9**[38] gives the bipyridine derivative **10**. Removal of the Boc-protecting group was successfully achieved with HCl in dioxane to give ligand **11**. The ethylene diamine linker in **11** allows for the covalent attachment of the Os complex to the polymer backbone by reaction of either the secondary or primary amino group with the epoxy functions at the polymer chain.

Exchange of the chloro ligands in **5** by **11** in ethylene glycol at 120 °C, followed by treatment with NH_4PF_6/water yields target complex **12** as the hexafluorophosphate salt. Cyclic voltammetry of **12** in in 0.15 M NBu_4PF_6/MeCN at a Pt disk electrode (Figure 1b) reveals a chemically reversible redox couple with $E_{1/2} = +0.13$ V (vs. Ag/Ag^+ 0.01 M $AgClO_4$), the differential pulse voltammogram of **12** (Figure S1, the Supporting Information) in the same electrolyte (note that due to the low solubility of **12** in water, characterization in aqueous electrolyte was not conducted) recorded with a pulse amplitude of 15 mV reveals a potential of maximum current (E_{max}) at +100 mV (vs. Ag/Ag^+ 0.01 M $AgClO_4$). The attachment of the $-NMe_2$ to the bpy-ligands leads to the envisaged low redox potential of the redox mediator.

Synthesis of the Os complex-modified redox polymer P-12

The copolymer backbone (terpolymer **P**) for the modification with the Os complex was synthesized (Scheme 3) from three monomers, that is, styrene, butyl acrylate, and allyl methacrylate, in a free radical polymerization reaction initiated by azobisisobutyronitrile (AIBN). In a post-polymerization reaction,

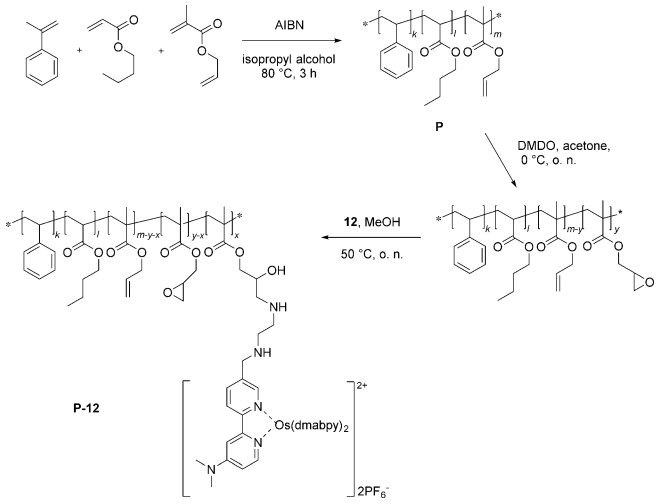

Scheme 3. Synthesis of redox polymer **P-12**. The terpolymer backbone (**P**) was obtained through a free radical polymerization reaction with AIBN as initiator (nominal composition of **P**: $k = 50$ mol%, $l = 35$ mol%, $m = 15$ mol%). Epoxidation of the allylic double bonds with dimethyldioxirane (DMDO) allows for a covalent attachment of the amino-modified Os complex **12**. Note that for **P-12** only the molecular structure of the product is shown, which is formed through the reaction of the primary amine in **12** and a single epoxy group in **P**. The nominal concentration of the Os complex within the modified polymer is expected to be <15 mol% because of non-quantitative conversion in each reaction step and potential multiple binding of the primary amino group to epoxy functions within the polymer.

the allyl groups were transformed into epoxides under mild conditions by means of dimethyl dioxirane (DMDO).[19] The epoxy groups allow for the covalent attachment of the Os complex **12** through a ring-opening reaction with the amino functions in **12** in a MeOH/isopropyl alcohol mixture at elevated temperatures. In the following the resulting polymer will be designated as **P-12**. Note that the binding of the complex may occur through the primary and the secondary amine in **12**. For clarity reasons, only the product from the reaction of the primary amine and one epoxy function is shown in Scheme 3.

The redox activity of the modified polymer **P-12** after drop-casting on an electrode surface was evaluated by means of cyclic voltammetry and differential pulse voltammetry (DPV) in aqueous electrolytes. Cyclic voltammograms (Figure 1c) of graphite electrodes coated with **P-12** by drop-casting show a chemically reversible redox couple with a half-wave potential of around $+30$ mV (scan rate $= 100$ mV s^{-1}, PBS buffer, pH 7.4). The DPV of **P-12** in 3 M KCl/water deposited onto a Pt electrode (Figure 1d) shows well-defined and pronounced peak with $E_{max} = +25$ mV (vs. Ag/AgCl 3 M KCl). From this value, a half-wave potential according to $E_{1/2} = E_{max} + (E_{pulse}/2)$ was derived to be $+32.5$ mV (with E_{pulse} = pulse amplitude in the DPV in mV). Note, that this value is shifted by about 70 mV to more cathodic potentials than that obtained for the freely diffusing complex **12** in the MeCN-based electrolyte ($+105$ mV vs. Ag/Ag$^+$ 0.01 M $AgClO_4$). This shift is identical to the potential difference between the aqueous electrolyte and the MeCN-based electrolyte observed for **5** (aqueous electrolyte: -0.70 V vs. Ag/AgCl 3 M KCl; MeCN-based electrolyte: -0.63 V vs. Ag/Ag$^+$ 0.01 M $AgClO_4$). The half-wave potential of **P-12** drop-cast onto a graphite electrode was estimated to be $+20$ mV (the Supporting Information, Figure S2). The applied synthetic strategy leads to a redox polymer with the envisaged redox potential close to 0 V versus Ag/AgCl 3 M KCl.

Enzyme electrodes and biocatalytic activity

To characterize the redox polymer **P-12** as immobilization matrix for the wiring of enzymes to electrode surfaces, graphite electrodes were modified with pyrroloquinoline quinone-dependent soluble glucose dehydrogenase (PQQ-sGDH) and **P-12** in the presence of 2,2′-(ethylenedioxy)diethanethiol acting as a crosslinker. The dithiol crosslinker ensures that stable films are formed on the electrode surface by reaction of the $-$SH groups with remaining epoxy functions of different polymer chains.[30] In the following, the enzyme is designated as PQQ-sGDH, whereas the enzyme integrated within the redox hydrogel is designated as PQQ-sGDH/**P-12**. PQQ-sGDH was chosen because it is insensitive to oxygen,[39,40] which is crucial for biosensors that operate under ambient conditions and for oxygen/glucose enzymatic biofuel cells. PQQ-sGDH shows an efficient mediated electron transfer in combination with Os complex-modified redox hydrogels.[30] The redox potential of PQQ-sGDH was reported to be -194 mV (vs. Ag/AgCl 3.5 M KCl, in the presence of Ca^{2+})[14,41] However, it depends strongly on the electrode material, pH value, presence of bivalent cations and/or presence of a redox mediator (see ref. [14] and references therein). As predicted, the redox potential of PQQ-sGDH is below that of **P-12** ($\approx +30$ mV vs. Ag/AgCl 3 M KCl) and hence a sufficient thermodynamic driving force exists for fast electron transfer from the enzyme to the electrode by electron hopping along the redox hydrogel.

Figure 2a shows the current response of PQQ-sGDH/**P-12**-modified electrodes prepared with different enzyme-to-polymer mass ratios of 1:1 (●), 1:2 (◆), 1:4 (■), 1:5 (▲) in the presence of increasing glucose concentrations and a constant applied potential of $+150$ mV versus Ag/AgCl 3 M KCl in 4-(2-hydroxyethyl)-1-piperazineethanesulfonic acid (HEPES) buffer (10 mM, pH 7, 0.1 vol.% Triton X-100). The PQQ-sGDH/**P-12**-modified electrodes show biocatalytic activity at comparatively low operating potential of $+150$ mV versus Ag/AgCl 3 M KCl (see the Supporting Information, Figure S3 for cyclic voltammograms of PQQ-sGDH/**P-12**-modified electrodes in presence and absence of glucose). Michaelis–Menten-type calibration graphs with apparent K_m values of 0.98 mM to 2.98 mM are obtained. The highest catalytic currents were obtained with a 1:4 enzyme-to-polymer ratio. In addition, the effect of different crosslinker loadings was studied. Figure 2b shows glucose cali-

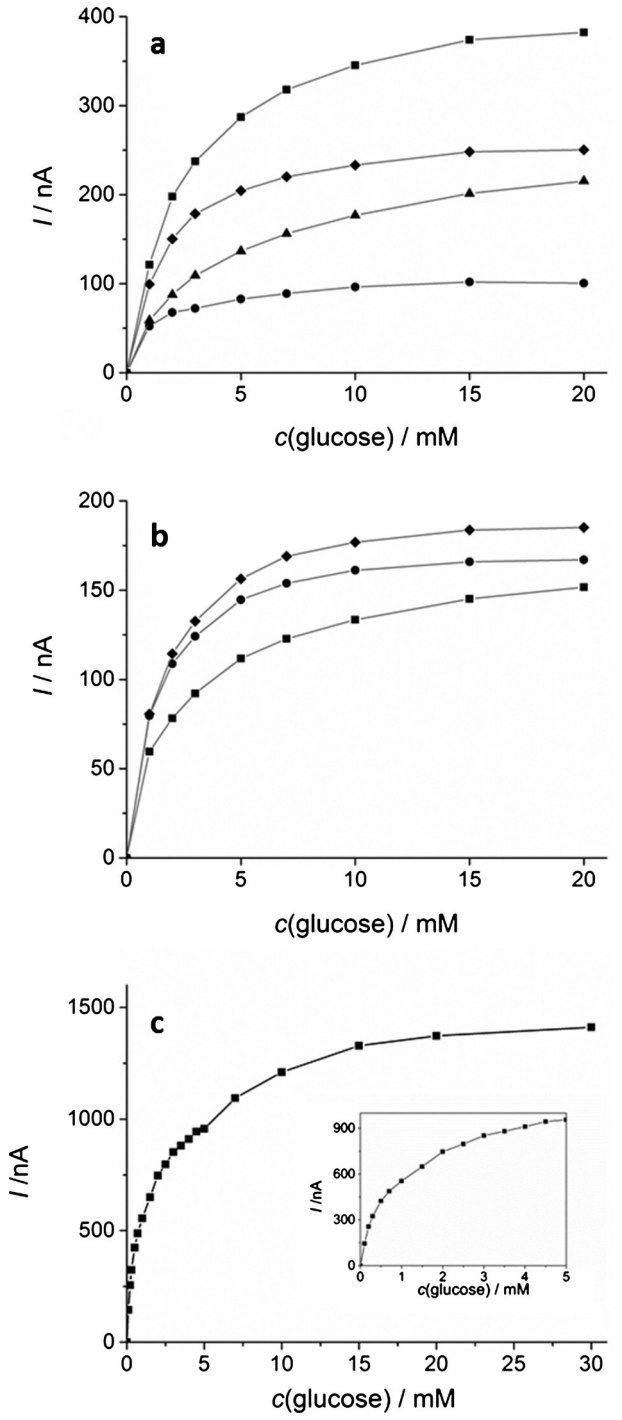

Figure 2. Biocatalytic activity of PQQ-sGDH/**P-12** films (on graphite electrodes, 3.05 mm) in dependence on the glucose concentration at an applied potential of +150 mV versus Ag/AgCl 3 M KCl; a) dependence of the catalytic current of PQQ-sGDH/**P-12** films prepared with different enzyme-to-polymer weight ratios 1:1 (●), 1:2 (◆), 1:4 (■), 1:5 (▲) in HEPES buffer (10 mM, pH 7, 0.1 vol.% Triton X-100); b) dependence of the catalytic current of PQQ-sGDH/**P-12** films prepared with different crosslinker loadings and constant enzyme-to-polymer ratio (1:4): 10.6 μg (●), 21.3 μg (◆), 31.9 μg (■) in HEPES buffer (10 mM, pH 7, 0.1 vol% Triton X-100); c) calibration curve of a PQQ-sGDH/**P-12** film in PBS buffer (pH 7.4, 1 mM $CaCl_2$); inset shows the current response in a concentration range of 0 to 5 mM. Lines are guidance for eyes only.

bration curves of PQQ-sGDH/**P-12** films (1:4) with different amounts of crosslinker used during drop-casting. The highest currents were obtained for a crosslinker-to-polymer mass ratio of ≈1:3.4. Interestingly, an increase of the temperature from room temperature to 30 °C and to 37 °C results in a decrease of the catalytic current (see Figure S4 in the Supporting Information), most likely due to desorption of the PQQ-sGDH/**P-12** films. Moreover, Sode et al. observed that the activity of PQQ-sGDH decreases at temperatures above 37 °C to 65%.[42] Dissolution or desorption of the film in combination with a reduced activity at elevated temperature may lead to the low catalytic currents obtained at 37 °C. Further experiments were performed at room temperature and with an enzyme-to-polymer mass ratio of 1:4 and a crosslinker-to-polymer mass ratio of 1:3.4.

The calibration curve (Figure 2c) for a PQQ-sGDH/**P-12** electrode in phosphate-buffered saline (PBS) with a pH 7.4 (1 mM $CaCl_2$) shows again a Michaelis–Menten-type behavior with an apparent K_M value of 1.74 mM. A limiting current is reached at concentrations above 5 mM. This behavior is in line with the results obtained in HEPES buffer (Figure 2a,b). A linear current response for low glucose concentration (0 to 5 mM) is, however, absent (inset in Figure 2c).

To evaluate the effect of parasitic oxygen reduction that was reported for Os complexes with redox potentials $< +70$ mV (vs. Ag/AgCl/3 M NaCl),[32] chronoamperometry experiments in HEPES buffer (10 mM, pH 7, 0.1 vol.% Triton X-100) and with a glucose concentration of 20 mM (saturation concentration) in the presence (air and oxygen atmosphere) and absence (argon atmosphere) of O_2 were conducted. Figure 3a shows the catalytic currents derived in Ar- (left column), O_2- (middle column), and air-saturated electrolyte solutions (right column) at an applied potential of +150 mV (vs. Ag/AgCl 3 M KCl). The current values in Ar- and air-saturated electrolytes reveal almost identical values of about 280 nA. The catalytic current is slightly higher for the O_2-saturated solution; however, the differences are small. Since parasitic oxygen reduction at the Os center should lead to decreased current values, we conclude that catalytic reduction at the suggested Os complex-modified polymer **P-12** is negligible.

The use of amperometric biosensors under physiological conditions is often hampered by interferences that occur because of the oxidation of electroactive substances at high operating potentials. Figure 3b shows the normalized catalytic currents at a glucose concentration of 30 mM in the absence and presence of electroactive interfering substances, that is, uric acid and ascorbic acid. The deviation of the normalized current, that is, the catalytic current in the presence of glucose and the interfering substance divided by the steady-state current that is obtained for only glucose was determined to be 1.03 for glucose/uric acid and 1.13 glucose/ascorbic acid. These results demonstrate the advantage of the low redox potential of the designed Os complex-modified redox hydrogel.

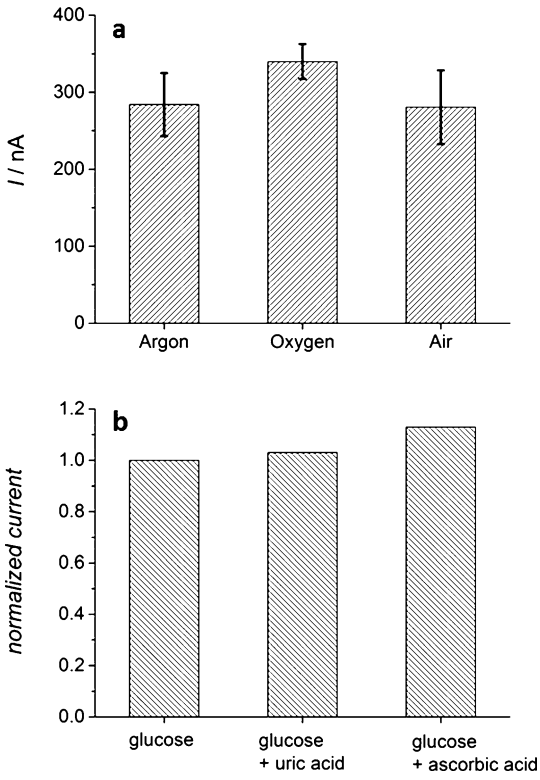

Figure 3. Effect of oxygen (a), uric acid and ascorbic acid (b) on the catalytic currents of PQQ-sGDH/**P-12**-modified graphite electrodes (3.05 mm) at glucose saturation concentration of 30 mM and an applied potential of +150 mV versus Ag/AgCl 3 M in HEPES buffer (10 mM, pH 7, 0.1 vol% Triton X-100); a) catalytic currents derived in different buffer solutions saturated with argon, oxygen and air; error bars are standard deviations from at least 3 independent measurements; b) Normalized catalytic currents derived for pristine glucose (=1) and in the presence of uric acid and ascorbic acid. Normalized currents were calculated by dividing the absolute steady state currents obtained in the presence of glucose and the interfering species by the steady state current that is obtained for only glucose.

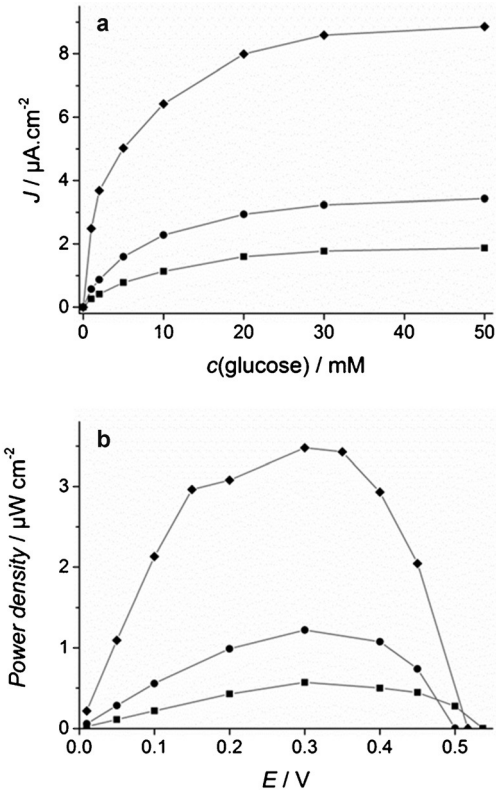

Figure 4. Biofuel cell characteristics of PQQ-sGDH/**P-12** (■), FAD-rGDH/**P-12** (●), and FAD-*Ct*CDH/**P-12** (▲)-modified graphite electrodes (3.05 mm). a) Current densities of the different **P-12**-based bioanodes in PBS (12 mM, pH 7.4, 0.14 M NaCl, 2.7 mM KCl); applied potential +150 mV (vs. Ag/AgCl/3 M KCl); b) dependence of the power densities on the operating voltage at a glucose concentration of 5 mM in PBS (12 mM, pH 7.4, 0.14 M NaCl, 2.7 mM KCl, for the experiments with PQQ-sGDH $CaCl_2$ (1 mM) was added to stabilize PQQ-sGDH) of the different bioanodes in combination with a *Mv*BOx-based biocathode (6 mm); all electrodes were prepared by drop-casting on graphite electrodes.

Anodes for enzymatic biofuel cells

Redox hydrogels with low formal potentials are of particular interest for enzymatic biofuel cells (EBFC) because the difference between the redox potential of the bioanode and biocathode determines the open circuit voltage of the resulting EBFC and hence should be maximal. Consequently, the application of **P-12** in combination with other glucose-dependent and O_2 tolerant enzymes, that is, flavin adenine dinucleotide-dependent recombinant glucose dehydrogenase (FAD-rGDH), and the flavodehydrogenase domain of cellubiose dehydrogenase from *Corynascus thermophilus* (FAD-*Ct*CDH), as well as PQQ-sGDH as potential anodes in biofuel cells was investigated.

Figure 4a shows the current density of graphite electrodes modified with films of PQQ-sGDH/**P-12**, FAD-rGDH/**P-12**, and FAD-*Ct*CDH/**P-12** at different glucose concentrations (0–50 mM) obtained at an applied potential of +150 mV (vs. Ag/AgCl 3 M KCl) in PBS buffer (pH 7.4). The highest current density is obtained with PQQ-sGDH followed by FAD-rGDH and FAD-*Ct*CDH.

Electrodes modified with PQQ-sGDH/**P-12**, FAD-rGDH/**P-12**, and FAD-*Ct*CDH/**P-12** films were used as bioanodes in a membrane-less biofuel cell together with a bilirubin oxidase (from *Myrothecium verrucaria*, *Mv*BOx)-based biocathode in PBS buffer solution at pH 7.4 containing glucose (5 mM). To ensure that the bioanode is limiting the EBFC, the area of the *Mv*BOx-modified cathode was substantially larger than the area of the bioanode. Figure 4b shows the dependence of the power density at different cell operating voltages. The highest power density is again achieved with the PQQ-sGDH/**P-12** couple. The EBFCs show open-circuit voltages (OCVs) between 0.50 V and 0.54 V as expected from the redox potentials of the **P-12** polymer (≈ +0.02 V at graphite electrodes) and that of the *Mv*BOx cathode (around +0.45 V).

Conclusion

An Os complex was designed envisaging stable N6 coordination, low redox potential due to stable electron-donating substituents at bpy ligands, and an amino-terminated linker chain for binding to epoxy-functionalities of a terpolymer backbone. A suitable Os complex was synthesized in a multi-step approach starting from simple precursors, that is, *N*,*N*′-dimethyl-

aminopyridin derivatives. The introduction of the $-NMe_2$ group in the ligand sphere of the Os complex ensures the envisaged low redox potential of around 0 V (vs. Ag/AgCl 3 M KCl). The covalent attachment of the Os complexes to the hydrogel was achieved by epoxidation of the polymer backbone and the reaction of the formed epoxy functions with amino groups within the ligand system of the Os species. The redox hydrogel could be successfully used as immobilization matrix for electrical wiring of various enzymes (PQQ-sGDH, FAD-rGDH, FAD-*Ct*CDH) to graphite electrodes. The modified electrodes were characterized with respect to their potential use as interference-free amperometric glucose sensors and as anodes in membrane-less glucose/oxygen enzymatic biofuel cells in combination with a bilirubin oxidase-based biocathode.

Evidently, the carefully designed low overpotential of the proposed redox polymer with respect of the PQQ-moiety in the active site of the enzyme is leading to a lower driving force for the electron transfer reaction between the enzyme and the polymer-bound redox mediator. Although higher current densities have been obtained previously with redox polymers bearing redox mediators exhibiting a higher formal potential, these higher current densities were obtained at the expense of a decrease of the open-circuit voltage of a related biofuel cell. In the case of a sensor application, a higher mediator potential is leading to cooxidation of potentially interfering compounds. Thus, although the power density and the biosensor activity/sensitivity of the proposed electrode architecture are lower as compared with those reported for other PQQ-sGDH-based enzyme electrodes that operate in a direct electron transfer mode[40,43] or in combination with different mediator species,[14,32,37,44–46] our results clearly demonstrate the advantage of an optimized redox potential preventing unintended electrochemical side reactions. The optimization/adjustment of the formal potential of the mediator with respect to a given enzyme and possible interferences is crucial for the design of improved enzyme-based biosensors and biofuel cells.

Experimental Section

Materials and methods

All materials and chemicals were purchased from Sigma–Aldrich, J.T. Baker, Acros Organics, VWR chemicals, Alfa Aesar or Applichem. Detailed protocols for the syntheses as well as characteristic analytical data for all compounds are given in the Supporting Information. The synthesis of 4,4′-bis-(*N*,*N*-dimethylamino)-2,2′-bipyridine was based on protocols described in ref. [36]. The synthesis of the amino-modified bipyridine ligand **11** was performed following protocols described in ref. [33] The synthesis of the copolymer backbone and the modification with the Os complex was based on procedures reported in ref. [19] Dimethyldioxirane (DMDO) was freshly prepared prior to use according to ref. [47].

4-(2-Hydroxyethyl)-1-piperazineethanesulfonic acid (HEPES) buffer (10 mM, pH 7.0) containing 0.1 vol.% Triton X-100 was prepared by dissolving HEPES in deionized water (Millipore) and adjustment of the pH value by addition of solid NaOH. Phosphate-buffered saline (PBS, 12 mM, pH 7.4) was prepared with Millipore water containing NaCl (0.14 M) and KCl (2.7 mM). The apo-enzyme of PQQ-dependent soluble glucose dehydrogenase (PQQ-sGDH) was a gift from Roche Diagnostics (Penzberg). Pyrroloquinolinequinone (PQQ) was purchased from Fluka. The apo-enzyme sGDH (1.08 mg) was reconstituted in 10 mM HEPES buffer (30 μL) containing 150 mM $CaCl_2$ (150 mM) and PQQ (500 μM) to form the holoenzyme PQQ-sGDH (incubation time 30 min, 4 °C). The activity of PQQ-sGDH was determined using a UV/Vis spectrophotometric assay containing 2,6-dichloroindophenol (DCIP). The absorption of DCIP was monitored at a wavelength of 600 nm. The activity of PQQ-sGDH was 3827 U mg^{-1}.

Flavin adenine dinucleotide (FAD)-dependent recombinant glucose dehydrogenase (rGDH) was prepared from *Glomerella cingulata* and was recombinantly expressed in *Pichia pastoris* (FAD-rGDH) as reported previously.[48] The protein concentration was 21 mg mL^{-1}, the specific activity of the enzyme was 793 U mg^{-1}.

The flavodehydrogenase domain of cellubiose dehydrogenase (CDH) from *Corynascus thermophilus* (FAD-*Ct*CDH) was prepared by recombinant production in *Pichia pastoris*.[49] The protein concentration and the specific activity were 16 mg mL^{-1} and 268 U mg^{-1}, respectively.

Bilirubin oxidase from *Myrothecium verrucaria* (*Mv*BOx) was obtained from Sigma–Aldrich. For electrode preparations, the enzyme (20 mg mL^{-1}) was dissolved in phosphate buffer (100 mM, pH 7) and drop-cast on the graphite surface.

Graphite electrodes were prepared from graphite rods (diameter 3.05 mm; SGL Carbon). The electrodes were polished with emery paper and subsequently sonicated for 5 min in water and in ethanol, respectively. The crosslinker, 2,2′-(ethylenedioxy)diethanethiol, was diluted in ethanol (1:50 v/v) prior to use. The redox polymer **P-12** (5 wt% in DMSO) was drop-cast on the electrode surface by means of a pipette (polymer amount 72 μg, 1.44 μL polymer suspension) and the electrode was left to dry in air. Then, enzyme (18 μg, dissolved in HEPES buffer, 10 mM, pH 7, 0.1 vol.% Triton X-100) and crosslinker (21.3 μg) were successively dropped on top of the polymer layer and mixed thoroughly on the electrode surface by means of a pipette tip. The modified electrodes were kept at 4 °C overnight to complete the crosslinking process. The modified electrodes were gently rinsed with water to remove loosely bound polymer and enzyme as well as remaining crosslinker. For biofuel cell tests, the biocathode was constructed by absorbing *Mv*BOx (800 μg) on a 6 mm graphite electrodes using a drop-cast process. The electrode was stored at 4 °C.

NMR experiments were conducted with a DPX 200 or a DRX 400 spectrometer from Bruker with ^1H resonance frequencies of 200.13 MHz and 400.13 MHz, respectively. UV/Vis absorption spectra were recorded with a Cary 60 absorption spectrometer from Agilent in quartz cuvettes (optical path length = 1 cm) in MeOH. MS spectra were recorded with VG Instruments Autospec (EI), Finnigan GCQ Iontrap (FAB) or a LTQ-Orbitrap XL spectrometer (ESI).

Electrochemical measurement

All electrochemical measurements were performed in a conventional three electrode set-up comprised of a graphite (diameter = 0.305 cm/surface area = 0.073 cm^2), platinum (1 mm/0.79 mm^2) or glassy carbon (0.3 cm/0.071 cm^2) working electrode, an Ag/AgCl 3 M KCl reference electrode and a Pt wire acting as counter electrode. Chronoamperometry was performed with a CHI1030 eight-channel potentiostat (CH Instruments) at an applied potential of +150 mV. All buffer solutions were purged with Ar for 15 min prior to the measurements. Differential pulse voltammetry (DPV) and cyclic voltammetry (CV) were used to investigate the redox potential of the redox polymer **P-12** using a three-electrode setup and potentiostats from PalmSens or CH Instruments. For experimental

details see the main text. Measurement parameters for DPV experiments: step potential = 5 mV; modulation amplitude = 15 mV; modulation time = 0.06 s and interval time 0.2 s. Cyclic voltammograms were recorded with a step potential of 1 or 2 mV at different scan rates (see main text). Half-wave potentials ($E_{1/2}$) determined from cyclic voltammetry were calculated from the peak potential in the forward (E_{pf}) and backward (E_{pb}) scan of the corresponding redox couples as $E_{1/2} = (E_{pf} + E_{pb})/2$. For cyclic voltammetry of **5**, the dichloro complex was suspended in EtOH and drop-cast onto the electrode surface (10–20 μL). The solvent was removed with a gentle argon stream.

Biofuel cell measurement

Biofuel cell tests were conducted in a one-compartment electrochemical cell using an Autolab PGSTAT12 potentiostat. The anode was connected as working electrode, whereas the cathode was connected as combined counter and reference electrode. To ensure that the anode is the limiting electrode in the biofuel cell, the geometric surface area of the cathode (0.28 cm^2) was always larger than that of the anode (0.073 cm^2).

Current and power density measurements were performed in PBS buffer (12 mM, pH 7.4, 0.14 M NaCl, 2.7 mM KCl) with a glucose concentration of 5 mM. In case of the PQQ-sGDH/**P-12** films $CaCl_2$ (1 mM) was added to the buffer solution to stabilize the PQQ-sGDH complex. For determination of the power output curves potential pulses in the range from 0 to 0.6 V (against open-circuit voltage) were applied and the current at each potential interval was recorded when a steady state was reached.

Acknowledgements

Financial support by the European Commission in the framework of the ITN "Bioenergy" (PITN-GA-2013-607793) and by the Deutsche Forschungsgemeinschaft in the framework of the Cluster of Excellence RESOLV (EXC 1069) is acknowledged. P.P. thanks the Deutscher Akademischer Austauschdienst (DAAD) for a PhD scholarship. The authors thank D. Wolters for ESI measurements.

Keywords: biosensors · hydrogel · osmium · polymers · redox chemistry

[1] A. Heller, *Curr. Opin. Chem. Biol.* **2006**, *10*, 664–672.
[2] K. Sirkar, M. V. Pishko, *Anal. Chem.* **1998**, *70*, 2888–2894.
[3] T. J. Ohara, R. Rajagopalan, A. Heller, *Anal. Chem.* **1994**, *66*, 2451–2457.
[4] D. A. Guschin, Y. M. Sultanov, N. F. Sharif-Zade, E. H. Aliyev, A. A. Efendiev, W. Schuhmann, *Electrochim. Acta* **2006**, *51*, 5137–5142.
[5] E. Suraniti, S. Tsujimura, F. Durand, N. Mano, *Electrochem. Commun.* **2013**, *26*, 41–44.
[6] F. Tasca, L. Gorton, M. Kujawa, I. Patel, W. Harreither, C. K. Peterbauer, R. Ludwig, G. Nöll, *Biosens. Bioelectron.* **2010**, *25*, 1710–1716.
[7] M. Shao, M. N. Zafar, M. Falk, R. Ludwig, C. Sygmund, C. K. Peterbauer, D. A. Guschin, D. MacAodha, P. Conghaile, D. Leech, M. D. Toscano, S. Shleev, W. Schuhmann, L. Gorton, *ChemPhysChem* **2013**, *14*, 2260–2269.
[8] T. Kothe, N. Plumeré, A. Badura, M. M. Nowaczyk, D. A. Guschin, M. Rögner, W. Schuhmann, *Angew. Chem. Int. Ed.* **2013**, *52*, 14233–14236; *Angew. Chem.* **2013**, *125*, 14483–14486.
[9] D. R. Baker, R. F. Simmerman, J. J. Sumner, B. D. Bruce, C. A. Lundgren, *Langmuir* **2014**, *30*, 13650–13655.
[10] A. Badura, D. Guschin, T. Kothe, M. J. Kopczak, W. Schuhmann, M. Rögner, *Energy Environ. Sci.* **2011**, *4*, 2435.
[11] P. Ó Conghaile, S. Pöller, D. MacAodha, W. Schuhmann, D. Leech, *Biosens. Bioelectron.* **2013**, *43*, 30–37.
[12] T. J. Ohara, R. Rajagopalan, A. Heller, *Anal. Chem.* **1993**, *65*, 3512–3517.
[13] D. A. Guschin, H. Shkil, W. Schuhmann, *Anal. Bioanal. Chem.* **2009**, *395*, 1693–1706.
[14] V. Flexer, N. Mano, *Anal. Chem.* **2014**, *86*, 2465–2473.
[15] D. A. Guschin, J. Castillo, N. Dimcheva, W. Schuhmann, *Anal. Bioanal. Chem.* **2010**, *398*, 1661–1673.
[16] U. Salaj-Kosla, M. D. Scanlon, T. Baumeister, K. Zahma, R. Ludwig, P. Ó. Conghaile, D. MacAodha, D. Leech, E. Magner, *Anal. Bioanal. Chem.* **2013**, *405*, 3823–3830.
[17] M. Shao, D. A. Guschin, Z. Kawah, Y. Beyl, L. Stoica, R. Ludwig, W. Schuhmann, X. Chen, *Electrochim. Acta* **2014**, *128*, 318–325.
[18] M. N. Zafar, F. Tasca, S. Boland, M. Kujawa, I. Patel, C. K. Peterbauer, D. Leech, L. Gorton, *Bioelectrochemistry* **2010**, *80*, 38–42.
[19] S. Pöller, Y. Beyl, J. Vivekananthan, D. A. Guschin, W. Schuhmann, *Bioelectrochemistry* **2012**, *87*, 178–184.
[20] H.-H. Kim, N. Mano, Y. Zhang, A. Heller, *J. Electrochem. Soc.* **2003**, *150*, A209–A213.
[21] P. Kavanagh, D. Leech, *Tetrahedron Lett.* **2004**, *45*, 121–123.
[22] H. Masui, A. B. P. Lever, *Inorg. Chem.* **1993**, *32*, 2199–2201.
[23] N. J. Ronkainen, H. B. Halsall, W. R. Heineman, *Chem. Soc. Rev.* **2010**, *39*, 1747–1763.
[24] A. Heller, B. Feldman, *Chem. Rev.* **2008**, *108*, 2482–2505.
[25] S. Calabrese Barton, J. Gallaway, P. Atanassov, *Chem. Rev.* **2004**, *104*, 4867–4886.
[26] Z. Gao, G. Binyamin, H.-H. Kim, S. C. Barton, Y. Zhang, A. Heller, *Angew. Chem. Int. Ed.* **2002**, *41*, 810; *Angew. Chem.* **2002**, *114*, 838.
[27] Y. Zhang, C. Ji, *Anal. Chem.* **2010**, *82*, 5275–5281.
[28] V. Soukharev, N. Mano, A. Heller, *J. Am. Chem. Soc.* **2004**, *126*, 8368–8369.
[29] F. Mao, N. Mano, A. Heller, *J. Am. Chem. Soc.* **2003**, *125*, 4951–4957.
[30] P. Pinyou, S. Pöller, X. Chen, W. Schuhmann, *Electroanalysis* **2015**, *27*, 200–208.
[31] W. D. Harman, D. P. Fairlie, H. Taube, *J. Am. Chem. Soc.* **1986**, *108*, 8223–8227.
[32] A. Prévoteau, N. Mano, *Electrochim. Acta* **2012**, *68*, 128–133.
[33] S. Pöller, W. Schuhmann, *Electrochim. Acta* **2014**, *140*, 101–107.
[34] F. Barrière, P. Kavanagh, D. Leech, *Electrochim. Acta* **2006**, *51*, 5187–5192.
[35] S. Murata, M. Miura, M. Nomura, *J. Chem. Soc. Chem. Commun.* **1989**, 116.
[36] D. Cuperly, P. Gros, Y. Fort, *J. Org. Chem.* **2002**, *67*, 238–241.
[37] K. Habermüller, A. Ramanavicius, V. Laurinavicius, W. Schuhmann, *Electroanalysis* **2000**, *12*, 1383–1389.
[38] M. A. Ghanem, J.-M. Chrétien, A. Pinczewska, J. D. Kilburn, P. N. Bartlett, *J. Mater. Chem.* **2008**, *18*, 4917–4927.
[39] L. Ye, M. Haemmerle, A. J. J. Olsthoorn, W. Schuhmann, H.-L. Schmidt, J. A. Duine, A. Heller, *Anal. Chem.* **1993**, *65*, 238–241.
[40] C. Tanne, G. Göbel, F. Lisdat, *Biosens. Bioelectron.* **2010**, *26*, 530–535.
[41] A. Sato, K. Takagi, K. Kano, N. Kato, J. A. Duine, T. Ikeda, *Biochem. J.* **2001**, *357*, 893–898.
[42] K. Sode, K. Watanabe, S. Ito, K. Matsumura, T. Kikuchi, *FEBS Lett.* **1995**, *364*, 325–327.
[43] I. W. Schubart, G. Göbel, F. Lisdat, *Electrochim. Acta* **2012**, *82*, 224–232.
[44] A. Malinauskas, J. Kuzmarskyt, R. Meskys, A. Ramanavicius, *Sens. Actuators B* **2004**, *100*, 387–394.
[45] J. Razumienė, V. Gurevičienė, V. Laurinavičius, J. V. Gražulevičius, *Sens. Actuators B* **2001**, *78*, 243–248.
[46] P. Pinyou, F. Conzuelo, K. Sliozberg, J. Vivekananthan, A. Contin, S. Pöller, N. Plumeré, W. Schuhmann, *Bioelectrochemistry* **2015**, *106*, 22–27.
[47] W. Adam, J. Bialas, L. Hadjiarapoglou, *Chem. Ber.* **1991**, *124*, 2377.
[48] C. Sygmund, P. Staudigl, M. Klausberger, N. Pinotsis, K. Djinović-Carugo, L. Gorton, D. Haltrich, R. Ludwig, *Microb. Cell Fact.* **2011**, *10*, 106.
[49] W. Harreither, A. K. G. Felice, R. Paukner, L. Gorton, R. Ludwig, C. Sygmund, *Biotechnol. J.* **2012**, *7*, 1359–1366.

Received: November 15, 2015
Published online on March 1, 2016